터널과 지하공간, 한국암반공학회
Vol. 13, No. 2, 2003, pp. 153~168

TUNNEL & UNDERGROUND Vol. 13, No. 2, 2003, pp. 153-168
J. of Korean Society for Rock Mech.

절리 발달 특성 및 심도 변화에 의한 방사성폐기물 처분장 주변영역에서의 열수리역학적 안정성 연구

김진웅[1], 배대석[1], 최종원[2]

Thermohydromechanical Stability Study on the Joint Characteristics and Depth Variations in the Region of an Underground Radwaste Repository

Jhinwung Kim, Daeseok Bae and Chongwon Choi

Abstract. The objective of this present study is to understand long term(500 years) thermohydromechanical interaction behavior in the vicinity of a repository cavern on the joint location and repository depth variations. The model includes a saturated discontinuous granitic rock mass, PWR spent nuclear fuel in a disposal canister surrounded with compacted bentonite inside a deposition hole, and mixed bentonite backfilled in the rest of the space within a repository cavern. It is assumed that two joint sets exist within the model. Joint set 1 includes joints of 56° dip angle, spaced at 20 m, and joint set 2 is in the perpendicular direction to joint set 1 and includes joints of 34° dip angle, spaced at 20 m. In order to understand the behavior change on the joint location variations, 5 different models of 500m in depth are analyzed, and additional 3 different models of 1000 m in depth are analyzed to understand the effect of depth variation.

KeyWords: Radwaste repository, Granite, Canister, Spent fuel, Bentonite, Deposition hole, Thermohydromechanical Interaction behavior, Backfill, Joint, Dip

초 록. 본 연구의 목적은 지하 고준위 방사성폐기물 처분공동 주변에서의 절리 위치 변화 및 처분공동의 지하 심도 변화에 따른 처분공동 및 주변 절리에서의 장기간(500년)에 걸친 열수리역학적 연성거동 변화를 분석하고, 앞으로 처분 개념 설정에 활용 하고자 하는 것이다. 해석모델은 포화된 불연속 화강 암반, 처분공내 압축 벤토나이트로 둘러쌓인 PWR 사용후 핵연료 및 처분용기, 그리고 처분동굴 내에 채워진 혼합 벤토나이트를 포함 한다. 해석모델 내에는 2개의 절리 세트가 존재하는 것으로 가정하였다; 절리세트1은 20 m 간격의 56도 경사의 절리들로 구성되었고, 절리세트 2는 절리세트 1에 수직방향으로 20 m 간격의 34도 경사의 절리들로 구성되었다. 절리 위치 변화의 영향을 파악하기 위하여 500 m 깊이의 모델 5개, 지하 심도 영향 파악을 위하여 추가로 3개의 1000 m 깊이의 모델을 해석하였다.

핵심어: 방사성폐기물 처분장, 화강암, 용기, 사용 후 핵연료, 벤토나이트, 처분공, 열수리역학적 연성거동, 뒷채움재, 절리, 경사

1. Introduction

To isolate high level radioactive materials from man and his environment, high level radioactive wastes are disposed of at a location very deep underground in a rock mass. A rock mass is one of the most important isolation barriers, especially granite being the most common and important repository host rock.

Granite masses are generally fractured in preferred directions, and the degree of fracturing decreases with increased depth. The matrix of a granitic rock mass is practically impermeable with a very low hydraulic conductivity. Hence, groundwater flows almost exclusively through the fractures. The hydraulic conductivity of a granitic rock mass depends on the

[1]한국원자력연구소 심부지질환경특성연구분야 책임연구원
[2]한국원자력연구소 처분시스템 개발분야 책임연구원
접수일: 2003년 3월 24일
심사 완료일: 2003년 4월 15일

degree of fracturing and on the interconnections between the fractures. For mechanical stability, the high strength of granitic rock enables high stability in underground openings in the rock masses. Thermal expansion of granite is low. However, thermal stresses may lead to microcracking due to different thermal expansions of the rock components and water inclusions. Thermal conductivity of granite is moderately good and rather independent from the temperature.

The assessment of coupling effects of rock mass stability, groundwater flow through a repository, external stresses, and thermal effects is an important part in the safety evaluation of a disposal system. The prediction of this coupled phenomena is also very important in planning and designing an underground opening in rock masses with discontinuities, such as fractures and faults, which show a significant effect on this coupled behavior.

State of the art studies on various coupled processes for rock joints have been summarized by Tsang (1990). For coupled thermal and mechanical behavior, the distinct element method has been used to analyze the behavior of the fractured rock masses for a radioactive waste repository(Shen et al, 1990). For coupled hydraulic and thermal behavior, the effect of increasing temperature, due to the decay heat of high level radioactive wastes, on the groundwater flow around a repository has been studied by many researchers(Hart, 1981; Noorishad et al, 1984). For coupled hydraulic, thermal, and mechanical behavior, Hart(1981) presented a model which fully describes the coupled behavior in nonlinear porous geological systems by an explicit finite difference method.

The objective of this present study is to understand long term(500 years) thermohydromechanical coupling behavior in the vicinity of a repository cavern on the variations of joint locations and repository depth.

2. Numerical model

2.1 High-level radioactive waste repository

High level radioactive wastes considered in this study are the PWR spent fuels cooled for the period of 40 years. Four assemblies of PWR spent fuels are emplaced in a hollow cylindrical canister, and then, fixed with a cast iron insert between the fuel assemblies and the canister.

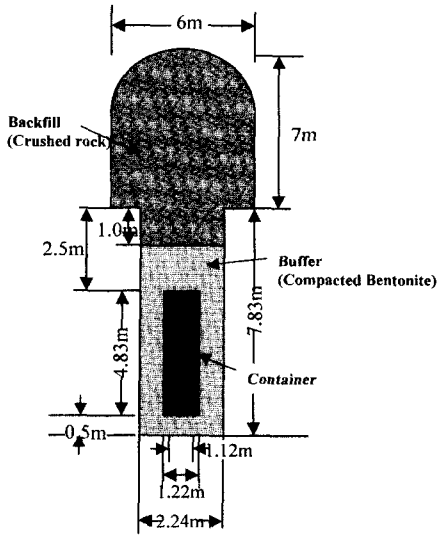

Figure 1. A cavern and a deposition hole with a canister.

The repository cavern is to be located deep underground in a granitic rock mass with discontinuities. The caverns are 250m long, spaced 40m apart, 6m wide, and have a vertical wall height of 4.5m and an arch shaped roof with a crown 7m above the cavern floor. Vertical deposition holes are located beneath the cavern floor along the centerline of the cavern at a pitch of 6 m. PWR spent fuels contained in cylindrical canisters are vertically emplaced in each deposition hole. Then, compacted bentonite buffer material fills the area between the canister and the surrounding rock mass, and backfill material, a mixture of bentonite and crushed rock, fills the rest of the space inside the cavern(Figure 1).

Radioactive materials in the PWR spent fuels generate decay heat through a radioactive decay process. The decay heat generated will influence the surroundings, such as the canisters, buffer and backfill materials, groundwater flow, adjacent rock mass, and the biosphere. Therefore, the behavior of a repository system should be analyzed for stability under the decay heat generated, H(T) in w/tHM(Kang, 2000):

$$H = 2201169e^{-5.205T}+1693.22e^{-0.018T}+124.7e^{-0.00058T} +19.134e^{-0.000042T}+1.429e^{-0.000001T} \quad (1)$$

where, T is the time after discharging PWR spent fuels, $0 \leq T \leq 10^6$ years.

2.2 Modeling

The models shown in Figures 2 to 9 are to simulate the coupled behavior of thermal, hydraulic, and mechanical interactions for a long term(500 years) behavior study of a repository. A 200m repository model is shown in Figures 2 to 4. There are two joint sets in the repository model; joint set 1 is 56° dip joints spaced 20 m apart, and joint set 2 is 34° dip joints spaced 20 m apart which are in the perpendicular direction to joint set 1. Five different models are shown in Figures 5 to 9, in which the location of the joints in joint set 1 is the same for all the five models, but in joint set 2 it changes for each model.

To simplify the analysis, a symmetry in the repository layout of multiple caverns in parallel with equal spacing has been utilized in the modeling. Horizontal boundaries are assumed far enough away from the

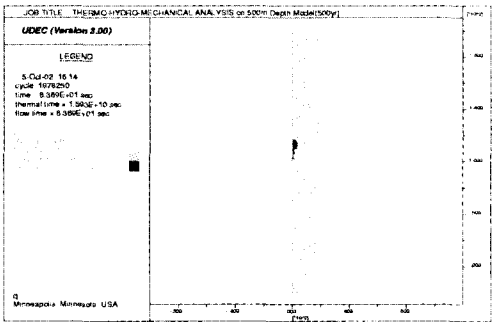

Figure 2. A model for a repository.

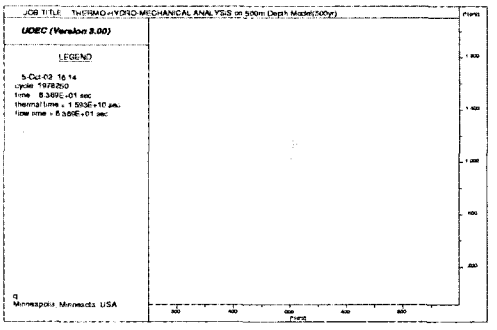

Figure 3. A 200m model for a repository with joints.

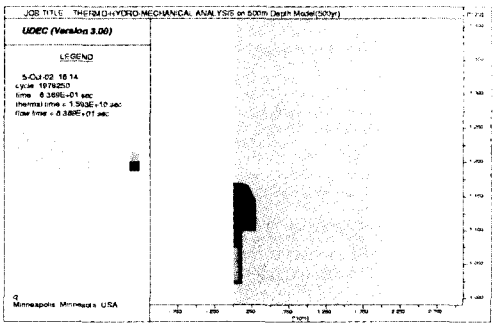

Figure 4. Enlarged view of a repository model showing a tunnel and a deposition hole with a canister.

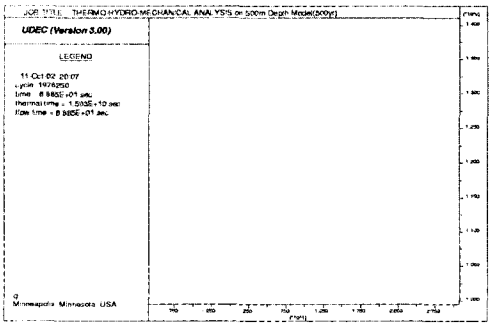

Figure 5. Enlarged view of the model a for a repository.

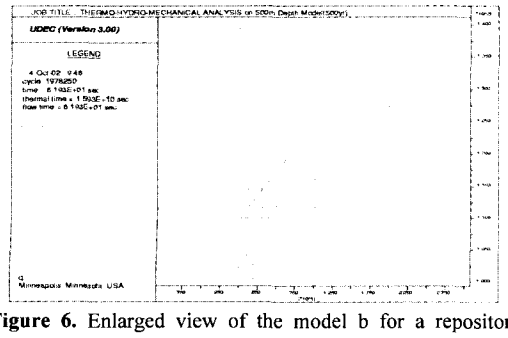

Figure 6. Enlarged view of the model b for a repository.

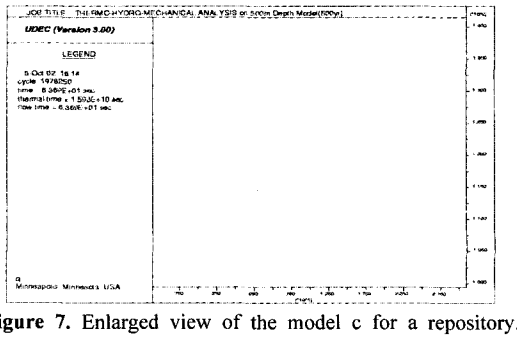

Figure 7. Enlarged view of the model c for a repository.

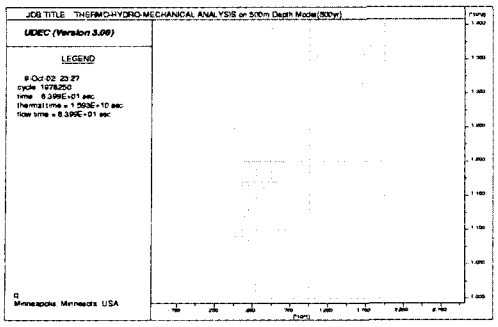

Figure 8. Enlarged view of the model d for a repository.

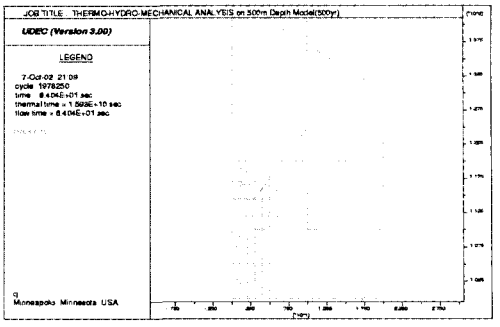

Figure 9. Enlarged view of the model e for a repository.

heat generating wastes at the top and bottom of the model. Excavation of the caverns, emplacement of the wastes, and filling of the buffer materials are all assumed to be instantaneous, and horizontal and vertical stresses are assumed to be equal initially.

Granitic rock mass is assumed to be homogeneous and isotropic satisfying Mohr-Coulombs elastoplastic failure criteria, and the compacted and mixed bentonite are regarded as elastoplastic material satisfying Drucker-Pragers failure criteria. The material for a canister is assumed to be homogeneous, isotropic, and linearly elastic. Barton-Bandis joint constitutive model is used for rock joints(Itasca, 1996).

The discrete waste location is distributed uniformly along the disposal cavern, in order to do a two dimensional approximation using the UDEC code. This means that a heat generating trench is located below the cavern floor along the centerline of the disposal cavern. After consideration of the tributary heating area of 10,000m^2 which is equal to the area of a cavern length of 250 m multiplied by a cavern spacing of 40m, heat flux, F, is then obtained from the equation (1),

$$F = (28.0554)e^{-(5.708E-10)t}+(4.1492)e^{-(1.839E-11)t} +(0.6486)e^{-(1.332E12)t}+(0.04876)e^{-(3.171E-14)t} \quad (2)$$

where, t is the time after 40 years of cooling, $0 \leq t \leq 3.1536E13$ sec, F in w/m^2.

For a hydraulic analysis using a steady state flow algorithm, groundwater flows through discontinuities in a rock mass. A fully coupled hydromechanical analysis is performed in which fracture conductivity is dependent on the mechanical deformation of a joint aperture; conversely, joint water pressures affect the mechanical behavior. Groundwater flow is governed by the hydraulic gradient differential between the adjacent domains. The cubic law for flow in a planar fracture is used in UDEC(Itasca,1996). The flow rate, q, from a domain with hydraulic pressure p_1 to a domain with hydraulic pressure p_2 is given by

$$q = -k_j a^3(\triangle p/l) \quad (3)$$

where k_j is a joint permeability factor whose theoretical value is $(1/12\,\mu)$, μ is the dynamic viscosity of the fluid, a is the contact hydraulic aperture, and l is the length assigned to the contact between the domains.

$$\triangle p = p_2-p_1+\rho_w g(y_2-y_1) \quad (4)$$

where ρ_w is the fluid density, g is the acceleration of gravity, and y_1,y_2 are the y-coordinates of domain centers.

The hydraulic aperture is given by

$$a = a_o + u_n \quad (5)$$

where a_o is the joint aperture at zero normal stress, and u_n is the joint normal displacement.

For a thermal analysis, this model simulates transient heat conduction in materials and the subsequent development of thermally induced displacements and stresses. Heat transfer is modeled as isotropic conduction and heat decays exponentially with time. The thermal analysis in UDEC(Itasca,1996) provides only one-way coupling to the mechanical stress calculation through

a thermal expansion coefficient and to the calculation for groundwater flow in joints through the temperature dependency of groundwater density and joint permeability. The basic equation of conductive heat transfer is Fourier's law.

$$Q_i = -k_{ij}(\partial T/\partial x_j) \quad (6)$$

where Q_i is the flux in the i-direction, k_{ij} is the thermal conductivity tensor, and T is the temperature. The change in temperature for any mass is as follows,

$$(\partial T/\partial t) = Q_{net}/(C_pM) \quad (7)$$

where Q_{net} is the net heat flow into mass, C_p is the specific heat, and M is the mass.

The equations (6) and (7) are the basis of the thermal version of UDEC. Temperature changes cause stress changes,

$$\triangle \sigma_{ij} = -\delta_{ij}\ 3\ K^*\ \alpha\ \triangle T \quad (8)$$

where $\triangle \sigma_{ij}$ is the change in stress ij, δ_{ij} is the Kronecker delta, K^* is K(for plane strain) and is equal to 6KG/(3K+4G) for plane stress, K is the bulk modulus, G is the shear modulus, α is the linear thermal expansion coefficient, and $\triangle T$ is the temperature change.

2.3 Initial and boundary conditions

Due to the symmetry in the repository layout of multiple caverns in parallel with an equal shape, length, and spacing, half of the repository is used in the model and symmetric boundary conditions are used. Boundary conditions for this fully saturated 200m model are fixed horizontal displacements on both sides, fixed vertical displacement at the bottom, and free at the surface. Impermeable boundary conditions are assumed on both sides and at the bottom of the model.

For thermal boundary conditions, it is assumed to be adiabatic on both sides and at the bottom. The temperature is assumed to be 20°C at the ground surface and to increase 0.6°C for every 20m below the surface. Therefore, the initial temperature is 32°C at the top and 38°C at the bottom of the model.

2.4 Material properties

Material properties for the host granitic rock, rock joint, compacted and mixed bentonite, and canister cast iron insert are shown in Tables 1 and 2(Kang et al, 2000; Hokmark et al, 1991; Hokmark, 1990; Johansson et al, 1991; SKB, 1997; SKB, 1997).

3. Results of the analysis

Five different models a, b, c, d, and e(Figures 5 to 9, in that order) at a depth of 500m are analyzed to study the effect of joint location variation. There are two joint sets in each model in which joint set 1 is 56° dip joints spaced 20m apart, and joint set 2 is 34° dip joints spaced 20m apart which are in the per-

Table 1. Mechanical and thermal properties of granite, compacted and mixed bentonite, and canister cast iron insert.

Parameter	Granite	Compacted bentonite	Mixed bentonite	Canister cast iron insert
Density, kg/m^3	2700	2100	2100	8000
Bulk modulus, Gpa	40	3.5	3.33	167
Shear modulus, Gpa	24	0.75	1.54	77
Thermal conductivity,				
W/mC	3.2	1.2	2	15.2
Thermal expansion				
coefficient, 1/°C	8.30E-06	0	8.30E-06	8.20E-06
Specific heat, J/kgC	815	1000	800	504
Friction angle, °	25			
Cohesion, Mpa	16			
Dilation	8			

Table 2. Mechanical properties of a joint set 1(56° dip angle) and a joint set 2(34° dip angle).

Parameter	Joint set 1	Joint set 2
Joint normal stiffness, Gpa/m	1.6E14	2.0E14
Joint shear stiffness, Gpa/m	2.0E13	2.3E13
Joint cohesion, Mpa	0.3	0.1
Joint dilation, °	0.0	0.0
Joint aperture, m	2.5E-3	1.0E-3
Joint permeability, 1/(Pa*sec)	1.0	3.0
Joint residual aperture, m	5.0E-5	5.0E-5
Joint roughness coefficient	7.0	5.0
Joint compressive strength, Mpa	30.0	30.0
Residual angle of friction, °	30.0	28.0
Intact rock compressive strength, Mpa	150.0	150.0

pendicular direction to joint set 1. In addition, three different models bk, ck, and dk at a depth of 1000m, which have the same mesh as that of the models b, c, and d, in that order, are analyzed to study the effect of depth variation.

3.1 Effect of joint location and depth variations

In-situ stresses are calculated for the 8 models mentioned above, and then, used for the next analyses, but displacements calculated are reset to zero values before the start of the next analysis. Distributions of vertical and horizontal components of insitu stresses, i.e., on a 500 m depth model, are shown in Figure 10 and 11. The insitu stresses on a 500m depth model are in the range from 11 MPa at the top to 16 MPa at the bottom of the model, while, the insitu stresses on a 1000 m depth model are in the range from 24 MPa at the top to 30 MPa at the bottom of the model.

The results of the analyses of each model are summarized in Tables 3 to 5 for three different stages; (1) after an instantaneous excavation of a repository cavern and a deposition hole, (2) after placing the canisters and buffer filling, and (3) after 500 years from waste emplacement.

In the stage after an instantaneous excavation in Table 3, a maximum crown displacement is 19.2 mm downward in model d among the models at a depth of 500 m, and 8.5 mm downward in model dk among the 1000 m depth models. A maximum displacement at a roof-wall intersection is 50.4 mm in model d and 17.6 mm in model dk directed toward an excavated space. A maximum shear displacement is 24.4 mm in model d and 15.6 mm in model dk. A minimum principal stress near a crown is -60.3 MPa in model d and -16.82 MPa in model dk. A minimum principal stress near a floor-wall intersection is -20.28 MPa in model d and -13.62 MPa in model dk.

In the stage after placing the canisters and buffer filling in Table 4, a maximum crown displacement is 21.2 mm downward in model d and 9.0 mm downward in model dk. Maximum displacements at the bottom of a deposition hole and at a roof-wall intersection

Table 3. Displacements and stresses on various models after an instantaneous excavation of a repository tunnel.

Results	Model a	Model b	Model c	Model d	Model e	Model bk	Model ck	Model dk
Displacement vector(mm)at crown	2.4	3.2	3.3	19.2	3.7	6.6	5.2	8.5
Displacement vector(mm) at bottom of deposition hole	1.4	1.7	2.3	9.4	2.0	3.3	3.7	7.8
Displacement vector(mm) at roof-wall intersection	6.1	4.5	7.5	50.4	8.4	10.0	11.2	17.6
Principal stress(MPa) near crown								
min.	-19.67	-17.07	-18.66	-60.30	-13.53	-32.79	-36.02	-16.82
max.	-4.54	-4.63	-4.56	-10.20	-4.27	-17.12	-9.45	-8.85
Principal stress(MPa) near floor-wall intersection								
min.	-4.80	-4.79	-5.16	-20.28	-10.58	-11.06	-16.09	-13.62
max.	-4.72	-4.75	-4.74	-6.82	-5.18	-9.82	-10.52	-11.25
Max. shear displacement(mm)	6.3	7.4	7.1	24.4	7.1	13.1	10.0	15.6

Table 4. Displacements and stresses on various models after placing canisters and buffer filling.

Results	Model a	Model b	Model c	Model d	Model e	Model bk	Model ck	Model dk
Displacement vector(mm) at crown	2.8	4.2	4.6	21.2	4.5	8.2	7.1	9.0
Displacement vector(mm) at floor center	2.2	2.4	0.9	0.3	0.4	4.1	0.6	0.7
Displacement vector(mm) at roof-wall intersection	1.1	1.2	1.7	11.5	2.1	2.6	5.8	9.0
Displacement vector(mm) at roof-wall intersection	6.9	6.2	8.7	51.6	10.4	11.9	15.6	20.0
Principal stress(MPa) near crown								
min.	-4.81	-17.47	-18.47	-55.58	-10.78	-32.88	-36.38	-21.54
max.	-4.64	-4.55	-4.56	-11.09	-4.39	-16.85	-9.46	-9.06
Principal stress(MPa) near floor-wall intersection								
min.	-4.85	-4.81	-4.92	-22.09	-8.07	-9.67	-12.97	-14.01
max.	-4.67	-4.77	-4.76	-6.26	-5.11	-9.61	-10.13	-9.89
Max. shear displacement(mm)	6.8	10.8	8.8	36.0	9.1	14.7	15.1	17.6

Table 5. Displacements and stresses on various models after 500 years from waste emplacement.

Results	Model a	Model b	Model c	Model d	Model e	Model bk	Model ck	Model dk
Displacement vector(mm) at crown	36.4	47.7	34.9	40.3	41.2	39.1	14.7	30.6
Displacement vector(mm) at floor center	34.0	47.4	33.9	39.6	49.4	39.3	30.7	30.7
Displacement vector(mm) at bottom of deposition hole	2.9	47.9	33.0	49.1	55.1	42.0	38.3	37.8
Displacement vector(mm) at roof-wall intersection	38.3	58.8	40.7	54.2	55.3	43.7	41.5	46.4
Principal stress(MPa) near crown								
min.	-6.75	8.16	-32.60	-58.61	-58.59	-37.03	-110.50	-48.87
max.	-5.61	13.52	-19.81	-13.47	-5.14	-18.17	-37.11	-9.19
Principal stress(MPa) near floor-wall intersection								
min.	-7.44	-57.72	-14.31	-26.60	-30.33	-40.95	-87.33	-19.43
max.	-4.87	-9.51	8.61	-12.63	2.98	-15.82	-37.08	-12.90
Max. shear displacement(mm)	7.7	26.2	7.9	35.0	25.5	17.2	22.8	26.0

are 11.5 mm upward and 51.6 mm directed toward a cavern, respectively, in model d, and 9.0 mm upward and 20.0mm directed toward a cavern, respectively, in model dk. A maximum shear displacement is 36.0mm in model d and 17.6 mm in model dk. From the results after an instantaneous excavation and after placing the canisters and buffer filling, shown in Tables 3 and 4, displacements and stresses on the 500 m depth model d are rather higher than those on the 1000 m depth model dk.

In the stage after 500 years from waste emplacement in Table 5, a maximum crown displacement is 40.3 mm upward in model d and 30.6mm upward in model dk. A maximum displacement at a roof-wall intersection is 54.2 mm upward in model d and 46.4mm upward in model dk. Minimum principal stresses near a crown and near a floor-wall intersection are -58.61 MPa and -26.60 MPa, respectively, in model d and

Table 6. Maximum displacements and stresses on a joint of 56° dip angle passing through a tunnel roof-wall intersection after an instantaneous excavation of a repository.

Results	Model a	Model b	Model c	Model d	Model e	Model bk	Model ck	Model dk
Max. vertical displacement(mm)	3.0	-2.3	2.96	-4.8	-2.0	-4.5	3.7	6.2
Max. horizontal displacement(mm)	-1.9	-1.5	-4.48	-20.5	-1.1	-3.2	-6.9	-12.0
Max. vertical stress(MPa)	-19.09	-13.25	-12.95	-49.06	-12.59	-28.32	-25.39	-28.22
Max. horizontal stress(MPa)	-24.88	-21.62	-21.0	-17.19	-12.85	-36.58	-37.92	-26.57
Max. shear stress(MPa)	7.57	4.74	5.07	2.66	3.15	8.42	9.06	6.01

Table 7. Maximum displacements and stresses on a joint of 56° dip angle passing through a tunnel roof-wall intersection after placing canisters and buffer filling.

Results	Model a	Model b	Model c	Model d	Model e	Model bk	Model ck	Model dk
Max. vertical displacement(mm)	2.9	-3.4	-3.7	-5.5	-2.5	-5.9	6.1	6.8
Max. horizontal displacement(mm)	-2.1	-2.2	-5.3	-21.7	-1.3	-3.4	-9.1	-14.1
Max. vertical stress(MPa)	-19.73	-13.73	-13.36	-43.51	-13.6	-29.18	-31.67	-30.13
Max. horizontal stress(MPa)	-25.22	-18.16	-21.26	-16.34	-13.09	-37.78	-43.28	-26.53
Max. shear stress(MPa)	7.75	1.42	4.83	2.89	2.97	9.0	11.09	15.13

Table 8. Maximum displacements and stresses on a joint of 56° dip angle passing through a tunnel roof-wall intersection after 500 years from waste emplacement.

Results	Model a	Model b	Model c	Model d	Model e	Model bk	Model ck	Model dk
Max. vertical displacement(mm)	48.0	94.0	53.5	60.5	97.4	59.2	70.3	43.0
Max. horizontal displacement(mm)	-6.1	3.5	-5.4	-29.0	7.4	-4.9	-21.1	-21.8
Max. vertical stress(MPa)	-17.85	-39.02	-19.47	-73.7	-15.63	-37.54	-101.16	-33.08
Max. horizontal stress(MPa)	-51.56	-37.82	-53.43	-38.42	-37.53	-58.07	-68.69	-53.02
Max. shear stress(MPa)	-4.98	-5.94	-18.17	-7.45	-12.54	-11.34	24.12	13.92

-110.5 MPa and -87.33 MPa, respectively, in model ck. A maximum shear displacement is 35.0 mm in model d and 26.0 mm in model dk. In the stage after 500 years from waste emplacement, stresses, in general, are higher in the 1000m depth models than in the 500m depth models, but displacements are larger in the 500m depth models.

In Tables 6 to 8, displacements and stresses on a 56° dip joint passing through a roof-wall intersection of various models are shown for three different stages. After an instantaneous cavern excavation shown in Table 6, horizontal displacements of 20.5 mm and 12.0 mm occur at a roof-wall intersection in models d and dk, respectively. After placing canisters and buffer filling, horizontal displacements of 21.7 mm and 14.1 mm occur at a roof-wall intersection in models d and dk, respectively(Table 7). After 500 years from waste emplacement, maximum horizontal displacement of 29.0 mm occurs at a roof-wall intersection of model d, and the maximum vertical displacements are 97.4 mm and 70.3mm near the end zone of a 56° dip joint farther away from a cavern in models e and ck, respectively. Maximum vertical and horizontal stresses of 101.16 MPa and 68.69 MPa, respectively, which are less than the intact rock compressive strength, occur in the location near a cavern roof-wall level of a 56° dip joint in model ck. From the results shown in Tables 6 to 8, stresses on a 56° dip joint, in general, are higher in the 1000 m depth models than in the 500m depth models, but a maximum horizontal displacement in a 56° dip joint occurs in the 500 m depth model d in all the stages mentioned above.

Therefore, it may be concluded, based on the present

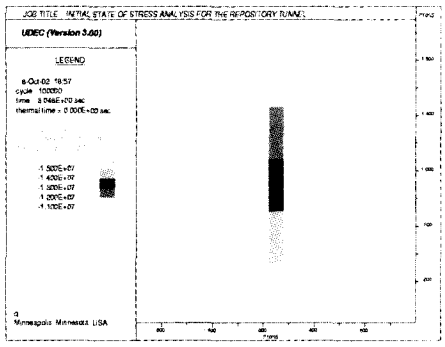

Figure 10. Distribution of a vertical component of an insitu stress on a 500m depth repository model.

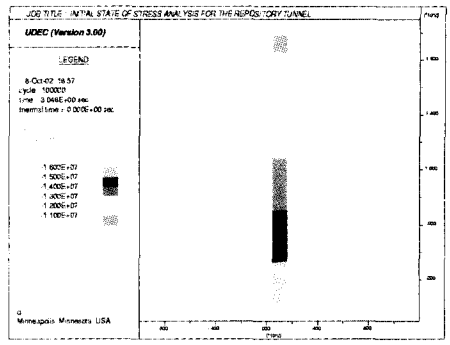

Figure 11. Distribution of a horizontal component of an insitu stress on a 500m depth repository model.

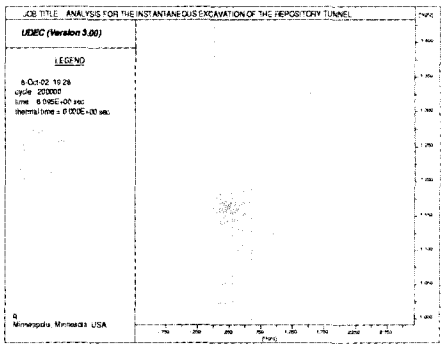

Figure 12. Enlarged view of the displacement distribution on a repository model after an instantaneous tunnel excavation.

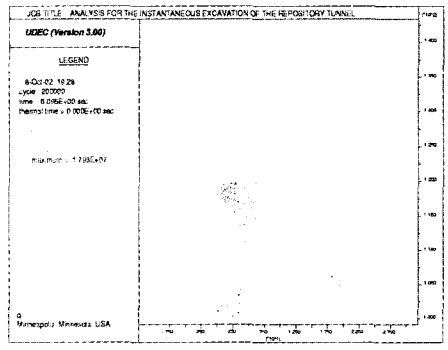

Figure 13. Enlarged view of the principal stress distribution on a repository model after an instantaneous tunnel excavation.

study, that the effect of a depth variation in the depth range from 500m to 1000m is not very important, and the effect of a joint location variation, on rocks and rock joints in the vicinity of a repository, is more important than the effect of a depth variation, and normal and shear displacement behavior is more important than stress behavior because magnitudes of the stresses obtained are well below a rock compressive strength.

3.2 Analysis of a 500m depth model with two joint sets

A 500m depth model d, in which one of the joints is passing slightly above the roof of a repository cavern, exhibits the highest normal and shear displacements compared to the displacements in the 500m depth models considered in the previous section (Tables 3 to 5). Hence, the 500m depth model d is studied further in order to understand long term(500 years) thermohydromechanical stability in the vicinity of a repository cavern.

3.2.1 After an instantaneous cavern excavation

The displacement and principal stress distributions in the vicinity of a repository model after an instantaneous excavation are shown in Figures 12 and 13. The cavern crown displaces 19.2 mm downward upon excavation. A maximum displacement occurs at a cavern roof-wall intersection and is 50.4 mm directed towards an excavated space, and a maximum shear displacement of 24.4 mm occurs near a cavern roof-wall intersection. The stresses are concentrated in the vicinity of a cavern after excavation. Minimum and maximum principal stresses near a cavern crown are -60.3 MPa and -10.2 MPa, and near a cavern floor-wall intersection are -20.28 MPa and -6.82 MPa, in that order(Table 3).

Maximum displacements and stresses on a 56° dip joint passing through a cavern roof-wall intersection are summarized in Table 6. Maximum vertical and

horizontal displacements are 4.8mm and 20.5 mm, respectively, and occur at a cavern roof-wall intersection. Vertical stresses are fairly uniformly distributed along the line of a joint and are -49.06 MPa, and the maximum horizontal and shear stresses of -17.19 MPa and 2.66 MPa occur near a cavern roof-wall intersection, respectively.

3.2.2 After placing canisters and buffer filling

It is assumed that the emplacement of radwastes and the filling of compacted and mixed bentonites are performed instantaneously. The distributions of displacements and principal stresses on a repository model after placing the canisters and buffer filling are in Figures 14 and 15. The cavern roof-wall intersection is displaced by 51.6 mm directed towards a backfilled cavern, and a cavern crown is displaced by 21.2 mm downward. A maximum shear displacement of 36.0 mm occurs near a cavern roof-wall intersection. Minimum and maximum principal stresses near a cavern crown are -55.58 MPa and -11.09 MPa, and near a cavern floor-wall intersection are -22.09 MPa and -6.26 MPa, in that order(Table 4).

Maximum displacements and stresses on a 56° dip joint passing through a cavern roof-wall intersection after canister emplacement and buffer filling are summarized in Table 7. Maximum vertical and horizontal displacements occuring at a cavern roof-wall intersection are 5.5 mm and 21.7 mm, respectively. Vertical stresses of -43.51 MPa are fairly uniformly distributed along the line of a joint, and maximum horizontal and shear stresses occur near a cavern roof-wall intersection and are -16.34 MPa and 2.89 MPa, respectively.

3.2.3 Long term behavior after waste emplacement

The long term(500 years) coupled thermohydromechanical interaction behavior is studied in this subsection. The displacement and principal stress distributions in the vicinity of a repository model after 500 years from waste emplacement are shown in Figures 16 and 17. The displacement at a cavern crown is 40.3 mm directed upward. Displacements at the floor center and at the bottom of the deposition hole are 39.6 mm and 49.1 mm directed upward, respectively. Maximum

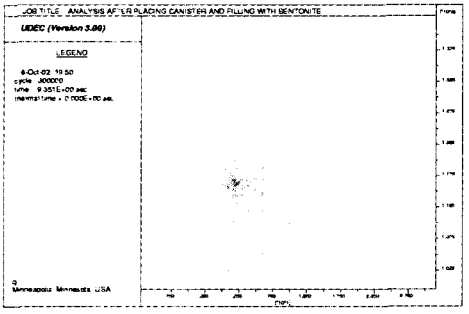

Figure 14. Displacement distribution on a repository model after placing canisters and buffer filling.

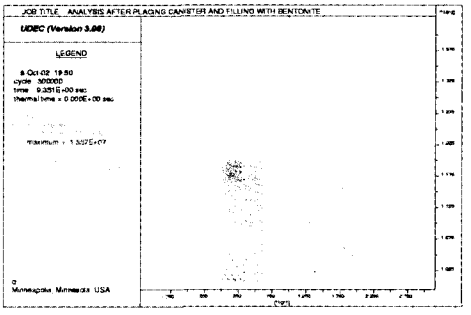

Figure 15. Principal stress distribution on a repository model after placing canisters and buffer filling.

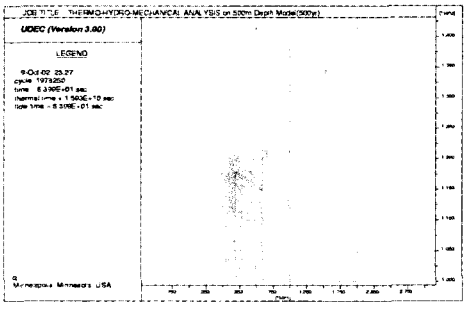

Figure 16. Displacement distribution on a repository model after 500 years from waste emplacement.

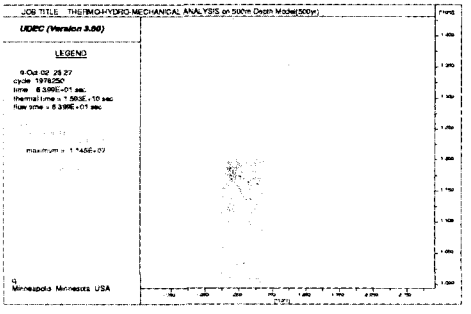

Figure 17. Principal stress distribution on a repository model after 500 years from waste emplacement.

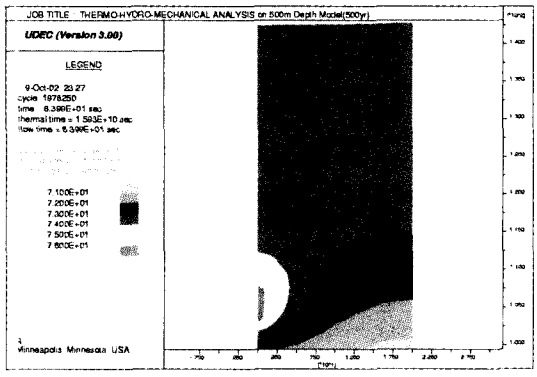

Figure 18. Enlarged view of the temperature distribution around a repository after 500 years from waste emplacement.

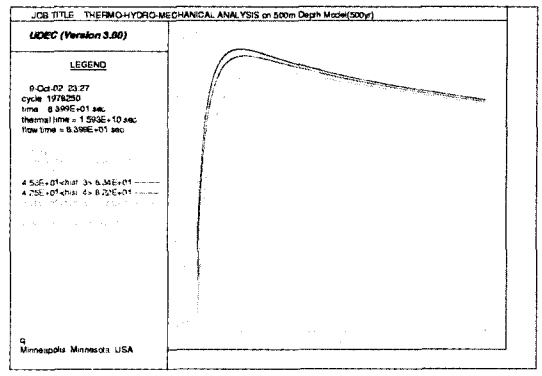

Figure 19. Temperature history at various locations on the tunnel of a repository for the period of 500 years from waste emplacement.

shear displacement of 35.0 mm occurs at the location, one cavern width away from the cavern wall on the level of a cavern floor. Minimum and maximum principal stresses near the cavern crown are -58.61 MPa and -13.47 MPa, and near the cavern floor-wall intersection are -26.6 MPa and -12.63 MPa, in that order.

Maximum displacements and stresses on a 56° dip joint passing through a cavern roof-wall intersection after 500 years from waste emplacement are shown in Table 8. Maximum vertical displacement is 60.5 mm directed upward in the far end zone from a cavern, and maximum horizontal displacement of 29.0 mm directed towards a cavern occurs at a cavern roof-wall intersection. Maximum shear displacement occurs on the joint at the level of the cavern crown and is 7.45 mm. Maximum vertical stress of -73.7 MPa occurs on the joint at the level of the cavern crown, and maximum horizontal stress of -38.42 MPa occurs in the far end zone from a cavern.

Temperature distribution around a repository after 500 years from waste emplacement is shown in Figure 18. The temperature distributions are roughly in the range from 76° C in a canister to 71° C further away from a canister after 500 years from waste emplacement. Figure 19 shows temperature histories at various locations in the repository model during the period of 500 years. The corresponding locations from the top in Figure 19 are the cavern floor center, deposition hole-cavern floor intersection, cavern floor-

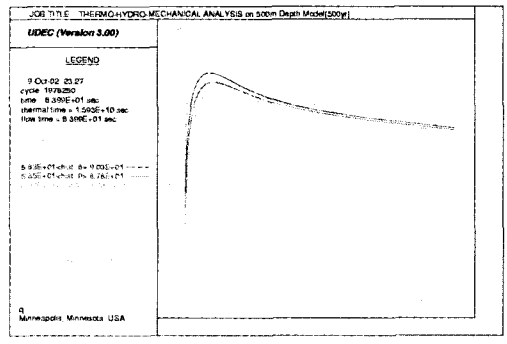

Figure 20. Temperature history at various locations along the horizontal line connecting the canister center on a repository model for the period of 500 years from waste emplacement.

wall intersection, cavern roof-wall intersection, and the cavern crown. The maximum temperatures at various locations are as follows: 83.5°C after 73 years from waste emplacement at the cavern floor center and at the deposition hole-cavern floor intersection, 82.2°C after 84 years from waste emplacement at the cavern floor-wall intersection, 79.5°C after 110 years from waste emplacement at the cavern roof-wall intersection, and 78.8°C after 140 years from waste emplacement at the cavern crown. The temperature distributions at the various locations mentioned above after 500 years from waste emplacement are asymptotically reduced and are in the range from 73.5°C to 74.5°C.

The temperature histories at various locations along

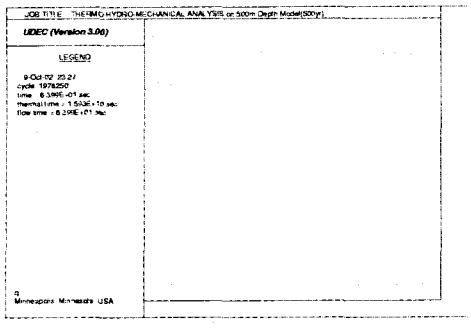

Figure 21. A vertical displacement history at a cavern crown during the period of 500 years from waste emplacement.

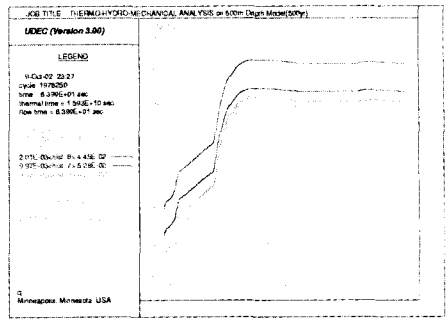

Figure 22. Vertical displacement histories at various locations around a cavern during the period of 500 years from waste emplacement.

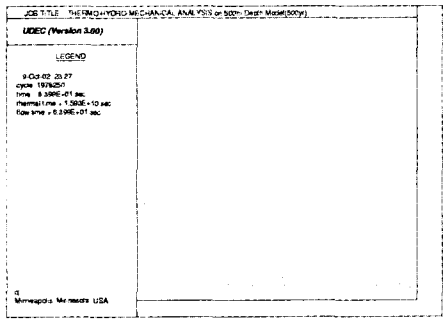

Figure 23. A vertical displacement history at a cavern roof-wall intersection during the period of 500 years from waste emplacement.

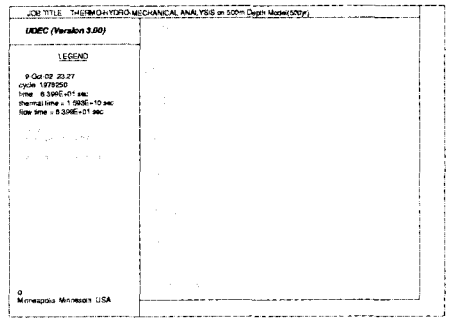

Figure 24. A horizontal displacement history at a cavern roof-wall intersection during the period of 500 years from waste emplacement.

the horizontal line connecting the canister center in the repository model during the period of 500 years are shown in Figure 20. The corresponding locations from the top in Figure 20 are the canister center, canister surface, deposition hole wall, 2 m, 3 m, 4 m, 5 m, 6 m, 10 m, 15 m, and 20 m away from the canister center. The maximum temperatures at various locations mentioned above are 95.8°C, 95.2°C, 90.3 °C, 87.8°C, 85.6°C, 84.0°C, 82.8°C, 81.9°C, 79.8°C, 78.5°C, and 78.3°C, in that order, and these maximum temperatures are reached after 30 to 100 years from waste emplacement, The temperature distributions at these locations after 500 years after waste emplacement are asymptotically reduced and are in the range from 71°C to 76°C.

During the period of 500 years from waste emplacement, the histories of the vertical and horizontal displacements are shown in Figures 21 to 24, and shear and normal stress histories are in Figures 25 and 26. A vertical crown displacement, as shown in Figure 21, is 3.7 mm downward after 16 years, and then, shows a fast increase to a maximum displacement of 41.9 mm upward after 200 years, and becomes 40.3 mm upward after 500 years from waste emplacement. Vertical displacement histories at various locations around a cavern are in Figure 22 showing similar behavior. Vertical displacements show fast increases for the first 200 years, and then, stay fairly constant for the rest of the period. Vertical and horizontal displacement histories at the cavern roof-wall intersection are shown in Figures 23 and 24. Shear and normal stress histories at a location 1m away from the cavern roof-wall intersection are shown in Figures 25 and 26. Shear and normal stresses show a lot of fluctuations for the first 30 years, and then, gradual increases in shear stress and decreases in normal stress up to 270 years, and then, they stay fairly constant, except for a small fluctuation at the

beginning, for the rest of the period.

The hydraulic aperture and flow rate variations along the line of a 56° dip joint passing through a cavern roof-wall intersection after 500 years from waste emplacement are shown in Figures 27 and 28. The maximum hydraulic aperture is 4.4E-3 m at the coordinate of (4.0 m,116.0 m), which is 1.7 m away from the cavern roof-wall intersection along the line of a 56° dip joint, and the flow rate at this coordinate is 1.0E-6 m^3/sec. The hydraulic aperture and flow rate at the coordinates of (6.0m, 120.0m) are 2.9E-3 m and 3.5E-7 m^3/sec, respectively, which are 5.3 m away from the cavern roof-wall intersection along the line of a joint. The hydraulic aperture and flow rate at the coordinates of (10.0m, 129.5m) are 1.7E-3 m and 2.25E-7 m^3/sec, respectively, which are 12.5 m away from the cavern roof-wall intersection along the line of a joint. The hydraulic aperture and flow rate at the coordinates of (15.0 m, 137.0 m) are 4.0E-4 m and 3.0E-8 m^3/sec, respectively, which is 22.0 m away from a cavern roof-wall intersection along the line of a joint. The hydraulic aperture and flow rate along the line of a joint stay constant beyond the coordinates of (15.0 m, 137.0 m). The changes in displacements and stresses in the vicinity of an underground cavern cause deformation and stress changes on joints adjacent to a cavern. Normal and shear displacements, and normal stress distributions on joints adjacent to a cavern show large variations in the region from a cavern wall to a radial distance away horizontally, and small variations in the next region to a diameter distance away horizontally from a cavern wall, and then, stay fairly constant beyond that region. Normal and shear deformations in joints and normal stresses acting in joints cause changes in joint aperture and joint permeability, and hence, influence groundwater flow.

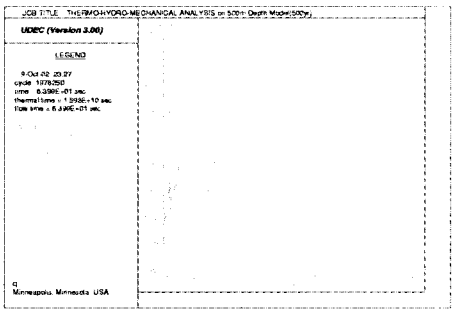

Figure 25. A shear stress history at a point of the coordinate of (4,114.5) during the period of 500 years from waste emplacement.

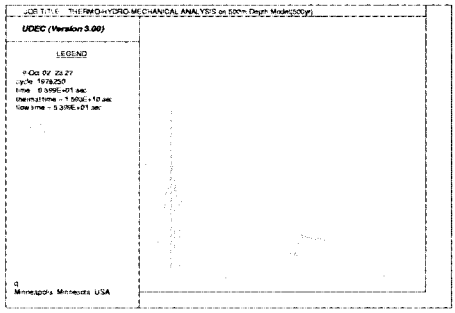

Figure 26. A normal stress history at a point of the coordinate of (4,114.5) during the period of 500 years from waste emplacement.

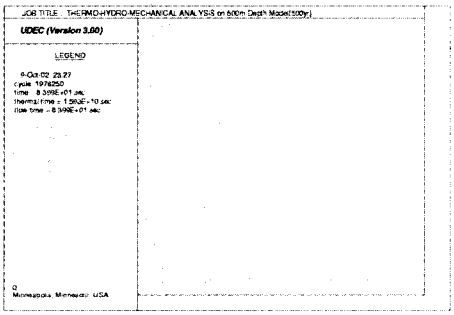

Figure 27. Hydraulic aperture variations along the line of 56o dip joint passing through a tunnel roof-wall intersection after 500 years from waste emplacement.

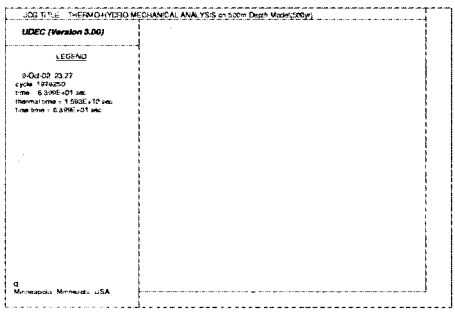

Figure 28. Flow rate variations along the line of 56o dip joint passing through a tunnel roof-wall intersection after 500 years from waste emplacement.

4. Conclusion

Long term(500 years) thermohydromechanical interaction behavior is studied in various repository models subjected to joint location and repository depth variations. The model includes a saturated discontinuous granitic rock mass, PWR spent nuclear fuels in a disposal canister surrounded by compacted bentonite inside a deposition hole, and mixed bentonite backfilled in the rest of the space within a repository cavern. It is assumed that two joint sets exist within a model. Joint set 1 includes joints of 56° dip angle, spaced 20 m apart, and joint set 2 is in the perpendicular direction to joint set 1 and includes joints of 34° dip angle, spaced 20 m apart.

Boundary conditions for this fully saturated 200 m model are fixed horizontal displacements on both sides, a fixed vertical displacement at the bottom, and free at the surface. Impermeable boundary conditions are assumed on both sides and at the bottom of the model.

For thermal boundary conditions, it is assumed to be adiabatic on both sides and at the bottom. The temperature is assumed to be 20°C at the ground surface and to increase 0.6°C for every 20 m below the surface. Therefore, the initial temperature is 32°C at the top and 38°C at the bottom of the model.

The two dimensional distinct element code, UDEC is used for the analysis. To understand the joint behavior adjacent to a repository cavern, the Barton-Bandis joint model is used. Effect of the decay heat for PWR spent fuels on a repository model has been analyzed, and a steady state flow algorithm is used for a hydraulic analysis.

Five different models a, b, c, d, and e(Figures 5 to 9, in that order) at a depth of 500 m are analyzed to study the effect of joint location variation. In addition, three different models bk, ck, and dk at a depth of 1000 m, which have the same mesh as that of models b, c, and d, in that order, are analyzed to study the effect of depth variation.

From the study of the effect of depth variation, the depth variation effect on structural behavior in a cavern and in the vicinity of a cavern differs in three different stages, namely, after an instantaneous excavation, after canister placement and buffer filling, and after 500 years from waste emplacement. In the stages after an instantaneous excavation and after placing the canisters and buffer filling, displacements and stresses are the largest in the 500m depth model d, in which a joint passes slightly above the cavern. In the stage after 500 years from waste emplacement, stresses, in general, are higher in the 1000 m depth models than in the 500 m depth models, but the magnitudes of stresses are less than an intact rock compressive strength. Displacements are larger in the 500 m depth models. Stresses on a joint, in general, are higher in the 1000 m depth models than in the 500 m depth models, but the maximum horizontal displacement on a joint occurs in the 500 m depth model d in all the stages.

From the study of the effect of joint location variation, the effect on structural behavior in a cavern and in the vicinity of a cavern differs to some degree in different models. In stages after an instantaneous excavation and after canister placement and buffer filling, displacements and stresses are much bigger in the model d than in other models. In the stage after 500 years from waste emplacement, displacements and stresses are large, but the differences in magnitudes of displacements and stresses are much reduced between models.

Therefore, it may be concluded, based on the assumptions of the present study, that the effect of depth increase in the depth range from 500 m to 1000 m is not very important, and the effect of decay heat is comparatively higher than the depth variation effect in the depth range mentioned. The effect of joint location variation, on rocks and rock joints in the vicinity of a repository, is more important than the effect of depth variation, and normal and shear displacement behavior is more important than the stress behavior because the magnitudes of the stresses obtained are fairly well below a rock compressive strength. The changes in displacements and stresses in the vicinity of an underground cavern cause deformation and stress changes in joints adjacent to the cavern. Normal and shear displacements, and normal stress distributions in joints adjacent to the cavern show large variations in the region from the cavern wall to

a radial distance away horizontally, and small variations in the next region to a diameter distance away horizontally from the cavern wall, and then, they stay fairly constant beyond that region. Normal and shear deformations in joints and normal stresses acting in joints cause changes in joint aperture and joint permeability, and hence, influence groundwater flow.

In planning and designing an underground opening in rock masses with discontinuities, it is advisable to do a thermohydromechanical stability analysis before locating an underground opening, especially, in the region of joint crossings.

Acknowledgment

The present study is financially supported by the National Long Term Nuclear R&D Fund from the Ministry of Science and Technology.

Reference

1. Tsang, C.F., 1990, *Coupling behavior of rock joints, in* Rock Joints(edited by N. Barton and O. Stephansson).
2. Shen, B. and O. Stephansson, 1990, Rock mass response to glaciation and thermal loading from nuclear waste, Proc. GEOVAL-90 Symp., Stockholm.
3. Hart, R.D., 1981, A fully coupled thermal-mechanical fluid flow model for nonlinear geologic system, PhD. Thesis, Univ. of Minn., Minnesota.
4. Noorishad, J., C.F. Tsang, and P.A. Witherspoon, 1984, Coupled thermal- hydraulic- mechanical phenomenon in saturated fractured porous rocks-numerical approach, J. Geophy. Res. 89.
5. Itasca Consulting Group, Inc.,1996, UDEC(Universal Distinct Element Code), version 3.0, Minneapolis, Minnesota.
6. Kang, C.H. et al, 2000, Preliminary conceptual design and performance assessment of a deep geological repository for high level wastes in the Republic of Korea, KAERI and Sandia National Lab., Rep. Of Korea.
7. Hokmark, H. and I. Israelsson, 1991, Distinct element modeling of joint behavior in nearfield rock, Stripa Project 91-22, SKB.
8. Hokmark, H., 1990, Distinct element method of fracture behavior in near field rock, Stripa Project 91-01, SKB.
9. Johansson, E., M. Hakala, and L.J. Lorig, 1991, Rock mechanical, thermomechanical, and hydraulic behavior of the near field for spent nuclear fuel, Report YJT-91-21, TVO, Helsinki.
10. SKB, 1997, Results from pre-investigations and detailed site characterizations: Summary Report, Aspo HRL-Geoscientific Evaluation 1997/2. SKB Technical Report 97-03.
11. SKB, 1997, Results from pre-investigations and detailed site characterization: Summary Report, Aspo HRL-Geoscientific Evaluation 1997/2, SKB Technical Report 97-04.

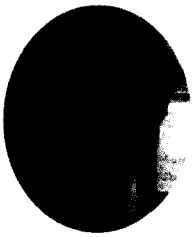

김 진 웅

1971년 Iowa State University, Civil Engineering, BS degree
1973년 University of Iowa, Structural Engineering, MS degree
1983년 Cornell University, Structural Engineering, PhD degree
Tel: 042-868-2018
E-mail: njwkim@kaeri.re.kr
현재 한국원자력연구소 심부지질환경특성연구분야 책임연구원

최 종 원

1984년 한양대학교 공과대학 원자력공학과 공학사
1992년 한양대학교 대학원 공과대학원자력 공학과 공학박사

Tel: 042-868-2041
E-mail: njwchoi@kaeri.re.kr
한국원자력연구소 처분시스템 개발 분야 책임연구원

배 대 석

1976년 경북대학교 문리과대학 지질학과 이학사
1990년 충남대학교대학원 지질학과 이학석사
1996년 충남대학교대학원 지질학과 이학박사
Tel: 042-868-2030
E-mail: ndsbae@kaeri.re.kr
현재 한국원자력연구소 심부지질환경특성연구분야 책임연구원